JYX
JYVÄSKYLÄN YLIOPISTO
UNIVERSITY OF JYVÄSKYLÄ

This is a self-archived version of an original article. This version may differ from the original in pagination and typographic details.

Author(s): Olito, Colin; de Vries, Charlotte

Title: The Demographic Costs of Sexually Antagonistic Selection in Partially Selfing Populations

Year: 2022

Version: Published version

Copyright: © 2022 the University of Chicago

Rights: CC BY-NC 4.0

Rights url: https://creativecommons.org/licenses/by-nc/4.0/

Please cite the original version:

Olito, C., & de Vries, C. (2022). The Demographic Costs of Sexually Antagonistic Selection in Partially Selfing Populations. American Naturalist, 200(3), 401-418. https://doi.org/10.1086/720419

The Demographic Costs of Sexually Antagonistic Selection in Partially Selfing Populations

Colin Olito[1,*] and Charlotte de Vries[2]

1. Department of Biology, Lund University, Lund 223 62, Sweden; 2. Department of Evolutionary Biology and Environmental Studies, University of Zurich, Zurich CH-8057, Switzerland; and Department of Biological and Environmental Science, University of Jyväskylä, FI-40014 Jyväskylä, Finland

Submitted June 4, 2021; Accepted March 1, 2022; Electronically published July 28, 2022

Online enhancements: supplemental PDF.

ABSTRACT: When selection differs between the sexes, genes expressed by both males and females can experience sexually antagonistic (SA) selection, where beneficial alleles for one sex are deleterious for the other. Classic population genetics theory has been fundamental to understanding how and when SA genetic variation can be maintained by balancing selection, but these models have rarely considered the demographic consequences of coexisting alleles with deleterious fitness effects in each sex. In this article, we develop a stage-structured Mendelian matrix model and jointly analyze the evolutionary and demographic consequences of SA selection in obligately outcrossing (i.e., dioecious/gonochorous) and partially selfing hermaphrodite populations. We focus on identifying when SA polymorphisms are maintained by balancing selection and the population growth rate remains positive. Additionally, we analyze the effects of inbreeding depression manifesting at different life history stages and give an illustrative example of the potential for SA polymorphism in real populations using empirically estimated demographic rates for the hermaphroditic flowering plant *Mimulus guttatus*. Our results show that when population intrinsic growth rates approach 1, extinction occurs across large swathes of parameter space, favoring SA polymorphism or the fixation of male-beneficial alleles, and that inbreeding depression is a significant problem for maintaining SA polymorphism in partially selfing populations. Despite these demographic challenges, our example with *M. guttatus* appears to show that demographic rates observed in some real populations can sustain large regions of viable SA polymorphic space.

Keywords: intralocus sexual conflict, evolutionary demography, partial selfing, inbreeding depression, polymorphism, *Mimulus guttatus*.

* Corresponding author; email: colin.olito@gmail.com.

ORCIDs: Olito, https://orcid.org/0000-0001-6883-0367; de Vries, https://orcid.org/0000-0001-8955-0479.

Introduction

A population's ability to adapt to its environment and persist in the long term depends on the genetic variation that it carries (Fisher 1930; Lewontin 1975). Yet populations are heterogeneous collections of individuals existing in a complex world where adaptation can be impeded by conflicting selection and gene flow between different classes of individuals (Charlesworth and Hughes 2000; Prout 2000; Connallon and Hall 2018).

Genetic constraints on adaptation due to conflicting selection have particularly interesting evolutionary consequences. On the one hand, they provide an effective mechanism for the maintenance of genetic variation, which shapes a population's capacity for future adaptation (Fisher 1930; Charlesworth and Hughes 2000; Prout 2000; Connallon and Hall 2018). On the other hand, they prevent individuals (or classes of individuals) from reaching their phenotypic optimum in one or more fitness components, which can increase a population's overall extinction risk (Kokko and Brooks 2003; Harts et al. 2014). Hence, for traits under conflicting selection, the nature and extent of genetic variation observed in natural populations should reflect a balance between the maintenance of genetic polymorphisms and the population dynamical consequences of the resulting maladaptation.

Sexually antagonistic (SA) selection is an important form of conflicting selection that occurs when beneficial alleles for one sex are deleterious when expressed in the other. Likewise, alleles with opposing fitness effects on male and female sex functions can experience SA selection in hermaphrodite populations, where individual fitness is determined jointly by maternal and paternal reproductive success (Lloyd and Webb 1986; Webb and Lloyd 1986;

American Naturalist, volume 200, number 3, September 2022. © 2022 The University of Chicago. This work is licensed under a Creative Commons Attribution-NonCommercial 4.0 International License (CC BY-NC 4.0), which permits non-commercial reuse of the work with attribution. For commercial use, contact journalpermissions@press.uchicago.edu. Published by The University of Chicago Press for The American Society of Naturalists. https://doi.org/10.1086/720419

Abbott 2011; Jordan and Connallon 2014). SA selection appears to be a common feature of sexually reproducing populations and is thought to contribute to the maintenance of genetic variation and the evolution of sexual dimorphism and sex-related traits (Kidwell et al. 1977; Lande 1980; Rice 1992; Charlesworth 1999; Rice and Chippindale 2001; Bonduriansky and Chenoweth 2009; Connallon and Clark 2012; Olito and Connallon 2019). For instance, sex differences in directional selection are commonly detected in phenotypic selection studies (e.g., Cox and Calsbeek 2009; Lewis et al. 2011; DeLisle et al. 2018; Singh and Punzalan 2018), suggesting that many genetic variants contributing to quantitative traits have SA effects. Moreover, quantitative genetic studies frequently find negative cross-sex genetic correlations for fitness (Chippindale et al. 2001; Delph et al. 2011; reviewed in Connallon and Matthews 2019), and polygenic signals of SA selection are evident in several recent population genetic analyses of large genomic data sets (Ruzicka et al. 2020, 2022). Overall, both theory and current empirical data suggest that there is ample scope for the maintenance of SA genetic variation in both dioecious (separate sexed) and hermaphrodite populations (Bonduriansky and Chenoweth 2009; Abbott 2011; Ruzicka et al. 2020; Wang et al. 2021).

While significant efforts have been made to predict when SA polymorphisms can be maintained and to detect SA genetic variation from empirical data, the demographic consequences of SA selection have often been overlooked (Matthews et al. 2019). Most population genetic theory, including SA selection theory, models the relative fitness of genotypes in populations of constant (and often infinite) size. In reality, these genotypic fitnesses emerge from myriad processes acting throughout the life history of individuals that link genotype distributions to population dynamics (e.g., Johnston et al. 2013; Mérot et al. 2020). For more than 50 years, the field of eco-evolutionary dynamics has sought to jointly model the genetic and demographic processes involved in evolutionary change. Theoretical models combining population genetics with density-dependent population growth (Roughgarden 1971) and stage-structured populations (consolidated in Charlesworth 1994) paved the way toward understanding the demographic consequences of allele frequency changes due to selection. Various extensions of these theories have been made to study life history evolution (Orive 1995, 2001), spatial structure (Rousset 2004), kin selection (Ronce et al. 2000), and quantitative trait evolution (e.g., Coulson et al. 2006; Barfield et al. 2011; Childs et al. 2016; Orive et al. 2017). This growing body of eco-evolutionary theory makes plain that demographic processes must be taken into account to fully understand how genetic variation for fitness is shaped in natural populations (Coulson et al. 2006; Rueffler et al. 2006; Metcalf and Pavard 2007).

The potential demographic costs of sexual antagonism were pointed out by Kokko and Brooks (2003), but few studies since have explicitly incorporated demography into models of sexual antagonism (with the notable exception of Harts et al. 2014). De Vries and Caswell (2019*b*) introduced a Mendelian matrix model with SA selection and population dynamics but did not analyze how demography influenced SA polymorphism. In this article, we extend the model of de Vries and Caswell (2019*a*, 2019*b*) to include both dioecious and hermaphroditic populations and jointly analyze the genetic (fixation/polymorphism) and demographic (persistence/extinction) outcomes of SA selection. A major strength of our approach is that the model can be parameterized using empirically estimated demographic rates, enabling us to make predictions about the scope of SA polymorphisms that are grounded in the biology of real populations. We demonstrate this with a case study of *Mimulus guttatus* (now *Erythranthe guttata*).

The Model

Here, we briefly describe a matrix model incorporating multiple life cycle stages and a single diallelic locus under SA selection on male and female fertility for populations of partially selfing simultaneous hermaphrodites. We focus our presentation on a two-stage example of the model and discuss its underlying biological assumptions. The derivation of the general model for any number of age or stage classes is provided in section S1 of the supplemental PDF. The derivation follows closely the logic presented in de Vries and Caswell (2019*a*, 2019*b*), and in fact it reduces to the two-sex stage-structured model of de Vries and Caswell (2019*b*) under obligate outcrossing (when selfing is not allowed). All computer code and data necessary to reproduce the results are available on Zenodo (https://doi.org/10.5281/zenodo.6021025; Olito and de Vries 2022) and GitHub (https://github.com/colin-olito/SA-Hermaphrodites-wDemography).

Simultaneous hermaphrodites can transmit genes to the next generation via both sperm/pollen and eggs/ovules, and they can potentially reproduce by a combination of self-fertilization and outcross fertilization. Maternal outcrossing involves receiving male gametes from other individuals in the population, while paternal outcrossing involves exporting male gametes to fertilize other individuals' ovules. Self-fertilization occurs when an individual's male gametes fertilize their own ovules. To distinguish between parameters relating to male and female reproductive functions, we denote matrices or vectors relating to the male sex function with a prime symbol. Following previous theory for partially selfing populations (e.g., Charlesworth and Charlesworth 2010; Jordan and Connallon 2014; Glémin 2021), we use a fixed prior selfing model where

all individuals are assumed to self-fertilize at a constant rate, C, prior to receiving outcross pollen. We present a more general model of genotype-specific self-fertilization rates in section S2 of the supplemental PDF and briefly discuss implications of this approach in the discussion section.

Individuals are jointly classified by life cycle stage $(1, \ldots, \omega)$, genotype $(1, \ldots, g)$, and whether they were produced by self-fertilization or outcross fertilization (denoted by S and X superscripts, respectively; see table 1 for a full description of terms included in the model). We include how individuals were produced in the state description because individuals produced by selfing might experience reduced survival, growth, or maturation rates as a result of inbreeding depression. This approach makes the common simplifying assumption that all individuals in the population experience the same severity of inbreeding depression (e.g., Charlesworth and Charlesworth 1987, 2010; Charlesworth and Willis 2009; Jordan and Connallon 2014). We address potential consequences of relaxing this assumption and how our model can be extended to do so in the discussion section.

The population state at time t is described by a population state vector, $\tilde{\mathbf{n}}(t)$, which is ordered by how individuals were produced (selfing vs. outcrossing), then by genotype, and finally by stage. For a single diallelic locus with alleles A and a, we have three genotypes (AA, Aa, aa; $g = 3$), giving the population state vector

$$\tilde{\mathbf{n}}(t) = \begin{bmatrix} \mathbf{n}^{\mathrm{S}}_{AA}(t) \\ \mathbf{n}^{\mathrm{S}}_{Aa}(t) \\ \mathbf{n}^{\mathrm{S}}_{aa}(t) \\ \hline \mathbf{n}^{\mathrm{X}}_{AA}(t) \\ \mathbf{n}^{\mathrm{X}}_{Aa}(t) \\ \mathbf{n}^{\mathrm{X}}_{aa}(t) \end{bmatrix}, \tag{1}$$

where $\mathbf{n}^{\mathrm{S}}_i$ and $\mathbf{n}^{\mathrm{X}}_i$ ($i \in \{AA, Aa, aa\}$) are the stage distribution vectors of individuals of genotype i produced by self-fertilization and outcrossing, respectively. The proportional population vector is given by

$$\tilde{\mathbf{p}}(t) = \frac{\tilde{\mathbf{n}}(t)}{\|\tilde{\mathbf{n}}(t)\|}, \tag{2}$$

where $\|\cdot\|$ is the one-norm. The population vector $\tilde{\mathbf{n}}(t)$ is projected forward from time t to $t + 1$ by the projection matrix $\tilde{\mathbf{A}}(\tilde{\mathbf{n}})$ such that

$$\tilde{\mathbf{n}}(t + 1) = \tilde{\mathbf{A}}[\tilde{\mathbf{n}}(t)]\tilde{\mathbf{n}}(t). \tag{3}$$

The population projection matrix $\tilde{\mathbf{A}}$ is constructed from four sets of matrices representing the demographic and genetic processes: the matrices $\mathbf{U}^{\mathrm{S}}_i$ and $\mathbf{U}^{\mathrm{X}}_i$ contain transition and survival probabilities for each genotype, produced by selfing and outcrossing, respectively. The matrices $\mathbf{F}_i$ and $\mathbf{F}'_i$ contain the genotype × stage–specific contributions of genotype i to the female and male gamete pools, respectively, and therefore to zygotes in the next generation.

Table 1: Mathematical notation and parameter values used in this article

Symbol	Definition	Dimension/value/range
	Symbols used in the general model description	
g	Number of genotypes (three; AA, Aa, and aa)	
ω	Number of stages (two; juvenile and adult)	
$\tilde{\mathbf{n}}$	Joint stage × genotype vector	$2\omega g \times 1$
$\tilde{\mathbf{p}}$	Joint stage × genotype frequency vector	$2\omega g \times 1$
$\mathbf{U}^{\mathrm{S}}_i$, $\mathbf{U}^{\mathrm{X}}_i$	Genotype-specific transition and survival matrices	$\omega \times \omega$
$\mathcal{U}^{\mathrm{S}}$, $\mathcal{U}^{\mathrm{X}}$	Block diagonal selfed/outcrossed survival matrices	$\omega g \times \omega g$
$\mathbf{F}_i$, $\mathbf{F}'_i$	Genotype-specific fertility matrices	$\omega \times \omega$
$\mathcal{F}^{\mathrm{S}}$, $\mathcal{F}^{\mathrm{X}}$	Block diagonal selfed/outcrossed fertility matrix	$\omega g \times \omega g$
q'_A, q'_a	Allele frequencies in male gamete pool	1
$\tilde{\mathbf{A}}(\tilde{\mathbf{p}})$	Population projection matrix	$2\omega g \times 2\omega g$
	Parameters used in the two-stage example	
s_{f}, s_{m}	Selection coefficients through female and male reproductive function	0–.15
h_{f}, h_{m}	Dominance coefficients through female and male reproductive function	1/2 or 1/4
σ_{j}, σ_{a}	Survival rates for juvenile and adult stages	.6
γ	Transition rate from juvenile to adult stages	.05
C	Population rate of self-fertilization	0–1
δ	Inbreeding depression effect on zygote viability	0–.8
δ_{j}	Inbreeding depression effect on juvenile survival	0–.8
δ_{a}	Inbreeding depression effect on adult survival	0–.8
δ_{γ}	Inbreeding depression effect on maturation rate	0–.8
f_i, f'_i	Adult maximum fertilities through female and male sex functions	5.8–8.5

We assume that whether individuals were produced through selfing or outcrossing does not affect their fecundity or mating success; that is, we assume $\mathbf{F}_i^{\mathrm{X}} = \mathbf{F}_i^{\mathrm{S}} = \mathbf{F}_i$ and $\mathbf{F}_i'^{\mathrm{X}} = \mathbf{F}_i'^{\mathrm{S}} = \mathbf{F}_i'$, respectively. Deviations from this assumption are straightforward to incorporate but beyond the scope of this article.

If the survival or fertility rates are a function of the population density, $\tilde{\mathbf{n}}(t)$, then the model will be density dependent and the population projection matrix becomes a function of the full population vector, $\tilde{\mathbf{A}}[\tilde{\mathbf{n}}(t)]$. Below, we limit our analyses to consider density-independent survival and fertility rates. The population projection matrix is then only a function of the proportional population vector, $\tilde{\mathbf{A}}[\tilde{\mathbf{p}}(t)]$, and the model is referred to as frequency dependent. In section S3 of the supplemental PDF, we construct and analyze a simple density-dependent version of the model and show that with density-dependent survival affecting all stages equally, our main conclusions remain intact.

SA Selection and Inbreeding Depression

We now construct and analyze an example genotype × stage–classified model for a hypothetical hermaphrodite species with intralocus sexual conflict via the two sex functions. For the sake of simplicity, we assume that our hypothetical species has a life cycle with only two stages, juveniles and adults (i.e., $\omega = 2$), and that only adults can reproduce. Suppose that there is a genetic trade-off between the sex functions at a single diallelic locus such that allele *A* is beneficial for female fertility but detrimental for male reproductive success (e.g., pollen production) and that allele *a* has the reverse effect. Following convention, we parameterize the fertility component of fitness for each genotype through each sex function, w_i and w_i', to be bounded by $[0, 1]$, with dominance and selection coefficients h_{f}, s_{f} and h_{m}, s_{m} determining the decrease in fertility through each sex function relative to the most fit genotype (*AA* has the highest female fertility, *aa* has the highest male fertility; see table 2).

The SA locus does not affect survival or transition rates. However, the survival matrices can be used to model the fitness effects of inbreeding depression at later stages of development by allowing different stage-specific survival and transition rates for individuals produced by self-fertilization versus outcrossing. By contrast, the parameter δ only affects inbreeding depression through viability of selfed ovules. With this in mind, we define survival matrices for individuals produced by selfing and outcrossing as follows:

$$\mathbf{U}^{\mathrm{S}} = \begin{pmatrix} \sigma_{\mathrm{j}}(1-\delta_j)(1-\gamma(1-\delta_\gamma)) & 0 \\ \sigma_{\mathrm{j}}(1-\delta_{\mathrm{j}})\gamma(1-\delta_\gamma) & \sigma_{\mathrm{a}}(1-\delta_{\mathrm{a}}) \end{pmatrix} \quad (4)$$

and

$$\mathbf{U}^{\mathrm{X}} = \begin{pmatrix} \sigma_{\mathrm{j}}(1-\gamma) & 0 \\ \sigma_{\mathrm{j}}\gamma & \sigma_{\mathrm{a}} \end{pmatrix}, \quad (5)$$

where σ_{j} and σ_{a} are the juvenile and adult stage survival rates, γ is the maturation rate from juvenile to adult stages, and the corresponding δ_{j}, δ_{a}, and δ_γ terms denote the proportional decreases in stage-specific survival and transition rates due to inbreeding depression (i.e., deleterious effects of inbreeding at later life history stages; e.g., Harder and Routely 2006). For simplicity, we assume that survival and transition rates are constant among genotypes.

Throughout our analyses, we distinguish between early- and late-acting inbreeding depression. We quantify early-acting inbreeding depression using δ and late-acting inbreeding depression using δ_i (where $i \in \{\mathrm{j}, \mathrm{a}, \gamma\}$). The term δ denotes the fraction of self-fertilized ovules that do not develop into juveniles because of inbreeding depression. An important difference between early- and late-acting inbreeding depression in the model is that δ affects the production of new individuals, whereas δ_i affects the demographic rates of extant individuals contained in $\mathbf{U}^{\mathrm{S}}$ (see eq. [4]).

The fertility matrices through female and male function are

$$\mathbf{F}_i = \begin{pmatrix} 0 & f w_i \\ 0 & 0 \end{pmatrix}, \quad (6)$$

and

$$\mathbf{F}_i' = \begin{pmatrix} 0 & f' w_i' \\ 0 & 0 \end{pmatrix}, \quad (7)$$

where f and f' represent maximum adult fertilities and w_i and w_i' represent the genotypic relative scaling factors for female and male sex functions (see table 2).

Unless stated otherwise, we use the following parameter values for the demographic rates in the model: $\sigma_{\mathrm{j}} = \sigma_{\mathrm{a}} = 0.6$ and $\gamma = 0.05$. These chosen values are similar to those used in de Vries and Caswell (2019*a*), facilitating comparison between models, and correspond to a life history in which individuals spend multiple time steps in the juvenile phase prior to maturing into reproductively active adults, but they are otherwise arbitrary. Our parameters of interest include maximum female fertility, f; the inbreeding depression parameters, δ, δ_{j}, δ_{a}, and

Table 2: Relative fertilities for sexually antagonistic selection (w_i)

	Genotype		
	AA	*Aa*	*aa*
Female function (w_i)	1	$1 - h_{\mathrm{f}}s_{\mathrm{f}}$	$1 - s_{\mathrm{f}}$
Male function (w_i')	$1 - s_{\mathrm{m}}$	$1 - h_{\mathrm{m}}s_{\mathrm{m}}$	1

δ_γ; and the selection parameters h_f, s_f, h_m, and s_m, which are given different values for each analyses as described in the figure legends.

Mating and Offspring Production under Partial Selfing

Outcrossing in our model proceeds similarly to a two-sex model of reproduction (de Vries and Caswell 2019*a*). That is, each individual's genotype determines both the number of ovules produced and the paternal mating success, broadly defined. For hermaphroditic flowering plants, for example, paternal mating success could reflect pollen production, export efficiency, and pollen tube germination and growth rates, among other things (Lloyd and Webb 1986; Harder et al. 2016; Wang et al. 2021). Note, however, that by modeling paternal relative mating success rather than pollen/sperm production, we make the common implicit assumption of female demographic dominance (i.e., population growth rates are determined by female fecundity, not production/transport of male gametes; Pollard 1975; Caswell 2001; Iannelli et al. 2005). We elaborate on several implications of this assumption for hermaphroditic populations in the discussion section.

For the purposes of this article, we assume that all outcross matings are random and that individuals produced by selfing or outcrossing have the same mating success, although they can differ in their survival (see above). Given these assumptions, the allele frequencies in the mating population can be obtained by summing the vectors of individuals produced through selfing and outcrossing:

$$\mathbf{p}' = \frac{(\mathbf{n}^{\mathrm{X}} + \mathbf{n}^{\mathrm{S}})}{\|(\mathbf{n}^{\mathrm{X}} + \mathbf{n}^{\mathrm{S}})\|}. \tag{8}$$

Individuals contribute gametes to the population outcrossing gamete pool according to their fertility, which depends on their stage and genotype at the SA locus. The allele frequencies in the male gamete pool are then calculated as

$$\begin{pmatrix} q'_A \\ q'_a \end{pmatrix} \propto \begin{pmatrix} 1^{\mathrm{I}}_\omega \mathbf{F}'_{AA}\mathbf{p}'_{AA} + \frac{1}{2}\mathbf{1}^{\mathrm{I}}_\omega \mathbf{F}'_{Aa}\mathbf{p}'_{Aa} \\ \frac{1}{2}1^{\mathrm{I}}_\omega \mathbf{F}'_{Aa}\mathbf{p}'_{Aa} + \mathbf{1}^{\mathrm{I}}_\omega \mathbf{F}'_{aa}\mathbf{p}'_{aa} \end{pmatrix}, \tag{9}$$

where equality is obtained by normalizing the frequencies such that they add to 1 (see sec. S1 of the supplemental PDF for a derivation of eq. [9]). The first entry sums the stage-specific contributions of allele *A* to the gamete pool by *AA* homozygotes and heterozygotes; the second entry does the same for the stage-specific contributions of allele *a* to the male gamete pool.

We now have all the ingredients to calculate the allele frequencies in the male gamete pool for the two-stage model in equation (7), equation (9), and table 2. Denoting the proportion of reproducing adults of genotype i with p_i^{R}, the allele frequencies in the male gamete pool are given by

$$\begin{aligned} \begin{pmatrix} q'_A \\ q'_a \end{pmatrix} &= \frac{1}{(1-s_m)p_{AA}^{\mathrm{R}} + (1-hs_m)p_{Aa}^{\mathrm{R}} + p_{aa}^{\mathrm{R}}} \\ &\quad \times \begin{pmatrix} (1-s_m)p_{AA}^{\mathrm{R}} + \frac{1}{2}(1-hs_m)p_{Aa}^{\mathrm{R}} \\ p_{aa}^{\mathrm{R}} + \frac{1}{2}(1-hs_m)p_{Aa}^{\mathrm{R}} \end{pmatrix}. \end{aligned} \tag{10}$$

Note that this equation is identical to the classical population genetic result for allele frequencies after selection among males in a two-sex SA model, with the caveat that only reproductively active adults contribute to the gamete pool (e.g., see eq. [1a] of Kidwell et al. 1977). However, equation (9) increasingly deviates from the classical population genetics result if additional reproductive stages are included.

Population Projection

Using the component matrices described above (the survival matrices, $\mathbf{U}_i^{\mathrm{X}}$, $\mathbf{U}_i^{\mathrm{S}}$, and the fertility and mating success matrices, $\mathbf{F}_i$, $\mathbf{F}_i'$) and the allele frequencies in the male gamete pool, we can construct the population projection matrix $\tilde{\mathbf{A}}[\tilde{\mathbf{n}}]$. The resulting matrix that projects the eco-evolutionary dynamics is

$$\tilde{\mathbf{A}}[\tilde{\mathbf{n}}] = \underbrace{\left(\begin{array}{c|c} \mathcal{U}^{\mathrm{S}} & 0 \\ \hline 0 & \mathcal{U}^{\mathrm{X}} \end{array}\right)}_{\tilde{\mathbf{U}}} + \underbrace{\left(\begin{array}{c|c} \mathcal{F}^{\mathrm{S}}(\tilde{\mathbf{p}})C(1-\delta) & \mathcal{F}^{\mathrm{S}}(\tilde{\mathbf{p}})C(1-\delta) \\ \hline \mathcal{F}^{\mathrm{X}}(\tilde{\mathbf{p}})(1-C) & \mathcal{F}^{\mathrm{X}}(\tilde{\mathbf{p}})(1-C) \end{array}\right)}_{\tilde{\mathbf{F}}}, \tag{11}$$

where C denotes the proportion of each individual's ovules that are self-fertilized (the remaining $1 - C$ are outcrossed) and δ represents the proportion of self-fertilized zygotes that fail to develop because of inbreeding depression during early development (Charlesworth and Charlesworth 1987).

The blocks of the component matrices in equation (11) correspond to production of offspring by self-fertilization and outcrossing ($\mathcal{F}^{\mathrm{S}}$ and $\mathcal{F}^{\mathrm{X}}$ in $\tilde{\mathbf{F}}$) and survival of extant individuals produced by selfing or outcrossing ($\mathcal{U}^{\mathrm{S}}$ and $\mathcal{U}^{\mathrm{X}}$ in $\tilde{\mathbf{U}}$). The survival matrices for individuals produced through selfing and outcrossing are

$$\mathcal{U}^{\mathrm{S}} = \begin{pmatrix} \mathbf{U}_{AA}^{\mathrm{S}} & \mathbf{0} & \mathbf{0} \\ \mathbf{0} & \mathbf{U}_{Aa}^{\mathrm{S}} & \mathbf{0} \\ \mathbf{0} & \mathbf{0} & \mathbf{U}_{aa}^{\mathrm{S}} \end{pmatrix}, \tag{12}$$

$$\mathcal{U}^{\mathrm{X}} = \begin{pmatrix} \mathbf{U}_{AA}^{\mathrm{X}} & \mathbf{0} & \mathbf{0} \\ \mathbf{0} & \mathbf{U}_{Aa}^{\mathrm{X}} & \mathbf{0} \\ \mathbf{0} & \mathbf{0} & \mathbf{U}_{aa}^{\mathrm{X}} \end{pmatrix}. \tag{13}$$

The survival matrices are block diagonal because individuals cannot change their genotype once they are born.

The fertility matrices for individuals produced through selfing and outcrossing are given by

$$\mathcal{F}^{\mathrm{S}} = \begin{pmatrix} \mathbf{F}_{AA} & \frac{1}{4}\mathbf{F}_{Aa} & \mathbf{0} \\ \mathbf{0} & \frac{1}{2}\mathbf{F}_{Aa} & \mathbf{0} \\ \mathbf{0} & \frac{1}{4}\mathbf{F}_{Aa} & \mathbf{F}_{aa} \end{pmatrix} \tag{14}$$

and

$$\mathcal{F}^{\mathrm{X}} = \begin{pmatrix} q'_A\mathbf{F}_{AA} & \frac{1}{2}q'_A\mathbf{F}_{Aa} & \mathbf{0} \\ q'_a\mathbf{F}_{AA} & \frac{1}{2}\mathbf{F}_{Aa} & q'_A\mathbf{F}_{aa} \\ \mathbf{0} & \frac{1}{2}q'_a\mathbf{F}_{Aa} & q'_a\mathbf{F}_{aa} \end{pmatrix}, \tag{15}$$

where q'_A and q'_a are the frequencies of alleles A and a in the gamete pool, given by equation (9).

The blocks of $\mathcal{F}^{\mathrm{X}}(\tilde{\mathbf{p}})$ can be constructed and interpreted as follows. The first row block of the first column produces AA offspring by outcrossing from AA maternal parents. This happens when the AA maternal parent receives an A gamete from the male gamete pool, which happens with probability q'_A. The other blocks can be interpreted similarly. Combining all the component matrices yields the overall eco-evolutionary projection matrix presented in section S1.3 of the supplemental PDF.

Iterating the projection matrix, equation (11), with the above-described demographic matrices, given an initial population state vector, allows numerical simulation of the eco-evolutionary dynamics for selection operating on any of the stage- or sex function–specific demographic parameters. As we outline below, we use numerical techniques together with mathematical analyses to study the conditions for the maintenance of SA polymorphisms and the demographic fate of the populations (i.e., positive growth or extinction).

Analyses

Diverse eco-evolutionary outcomes are possible in the model, including fixation of either allele, balanced polymorphism, population growth or extinction, and even evolutionary rescue and suicide (for examples of the possible outcomes, see de Vries and Caswell 2019*a*, 2019*b*). We focus on identifying parameter conditions where two criteria are satisfied: (i) SA polymorphism is maintained under balancing selection (fig. 1, *left*) and (ii) the intrinsic population growth rate at equilibrium, λ, is greater than 1 (fig. 1, *right*). It is a situation we refer to as a "demographically viable SA polymorphism."

We identify conditions where SA polymorphism is "protected" by evaluating the stability of populations initially fixed for either allele to invasion by the other (i.e., we assessed stability at the boundary equilibrium genotype frequencies of $\hat{\mathbf{p}}_{AA} = 1$ and $\hat{\mathbf{p}}_{aa} = 1$; Levene 1953; Prout

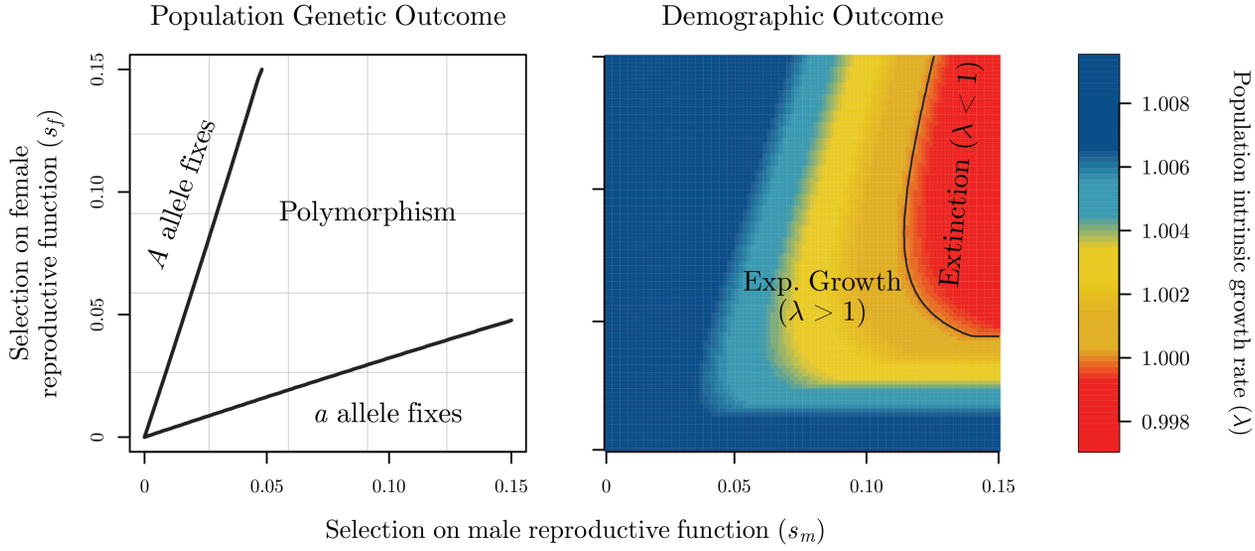

Figure 1: Illustration of the possible population genetic outcomes of the model on the left (fixation of either allele or a polymorphism) and of our demographic outcome of interest on the right (population growth rates). For clarity, results are shown for the case of a dominance reversal, where $h_{\mathrm{f}} = h_{\mathrm{m}} = 1/4$.

1968; de Vries and Caswell 2019*a*). The formal conditions for a protected polymorphism are determined by linearizing the model in the vicinity of the boundary equilibria ($\hat{\mathbf{p}}$) and evaluating the magnitude of the largest eigenvalue of the Jacobian matrix of the linearization. A full derivation of the Jacobian, details of the invasion analysis, and the relevant leading eigenvalues are presented in section S2 of the supplemental PDF.

We used numerical simulation to determine whether a protected SA polymorphism was also demographically viable. Specifically, for each boundary equilibrium we introduced the rare allele at low initial frequency and iterated equation (11) until the population had reached demographic and genotypic equilibrium. Although we use density-independent survival and fertility rates, the allele frequency dynamics introduce frequency dependence into the model. The population state vector will therefore grow or shrink exponentially after converging to stable population structure and genotypic frequencies (see Caswell 2001, chap. 17). The intrinsic population growth rate after convergence, λ, can be calculated as $n(t)/n(t+1)$, where $n = \sum_i n_i$ sums over all entries of the population state vector $\tilde{\mathbf{n}}$.

Because single-locus selection coefficients are generally weak (e.g., Eyre-Walker and Keightly 2007) and strongly skewed, we limit our analyses to coefficients within $0 < s_f, s_m \leq 0.15$, unless stated otherwise. We present scenarios of equal dominance in the main text (i.e., $h_f = h_m = h$). Specifically, we examine scenarios of (i) additive SA fitness effects ($h = 1/2$), which are commonly observed for small-effect alleles or quantitative traits (Agrawal and Whitlock 2011), and (ii) dominance reversals, where the deleterious fitness effect of each SA allele is partially recessive through each sex function ($h = 1/4$), which are predicted under fitness landscape models provided the population is not too far from the phenotypic optimum (Manna et al. 2011; Connallon and Clark 2014). We briefly explore the consequences of sex-specific dominance in section S4 of the supplemental PDF.

To analyze the demographic effects of inbreeding depression, we make two additional simplifying assumptions. First, to keep our analyses tractable we explore the effects of individual inbreeding depression terms in isolation. That is, we assume that only one of the δ and δ_i terms (where $i \in \{j, a, \gamma\}$) can be nonzero at a time. Second, we assume that if inbreeding depression is caused primarily by recessive deleterious mutations (as suggested by empirical data), it should covary negatively with the population selfing rate due to purging, provided the population selfing rate has been relatively constant in recent evolutionary time (Charlesworth and Willis 2009; although we note that other processes could give rise to this pattern, e.g., Crnokrak and Barrett 2002; Charlesworth and Willis 2009; Hedrick and Garcia-Dorado 2016). Following Olito and Connallon (2019), we incorporate such negative covariance by constraining the inbreeding depression terms in the model (δ and δ_i, where $i \in \{j, a, \gamma\}$) to follow a simple declining function of the selfing rate:

$$\delta = \delta^* \left(1 - b\left(1 - \frac{a(1-C)}{(C + a(1-C))}\right)\right), \qquad (16)$$

where δ^* is the hypothetical severity of inbreeding depression for a completely outcrossing population, b is a shape parameter determining how far δ will decline under complete selfing (when $C = 1$), and a is a shape parameter controlling the curvature of the overall function for δ (for additional details, see app. E in Olito and Connallon 2019). We set $\delta^* = 0.8$, $b = 0.5$, and $a = 0.2$ for all analyses involving inbreeding depression, values chosen to be consistent with empirical estimates of inbreeding depression (e.g., fig. 2 in Husband and Schemske 1996).

Results

Fixation, Polymorphism, and Extinction

We begin with an illustration of demographically viable polymorphic parameter space in the absence of inbreeding depression in figure 2 (i.e., $\delta = \delta_i = 0$). The red regions in figure 2 indicate areas where the population becomes extinct (i.e., where $\lambda < 1$) for different maximum female fertility values. Lower female fertility values correspond to larger areas where extinction occurs. The funnel between the thick black lines indicates the area where the SA alleles coexist. Above the funnel, the female-benefit/male-detriment allele goes to fixation; below the funnel, the male-benefit/female-detriment allele goes to fixation. Much of the region where the male-benefit/female-detriment allele fixes is demographically inviable because of the demographic consequences of reduced female fertility in this region. The SA polymorphisms that remain viable at lower fertility values correspond to regions where the female-deleterious allele is predicted to segregate at low frequencies or to regions with weak selection through both sex functions, an asymmetry that reflects the assumption of female demographic dominance.

Invasion conditions for SA alleles in the evolutionary demographic model closely match the predictions from population genetic models (Kidwell et al. 1977; Jordan and Connallon 2014; Olito 2017). In particular, the demographic model recovers the classic funnel-shaped region of polymorphic $s_f \times s_m$ parameter space. The effects of the population selfing rate (C) and dominance (h) on SA polymorphism are also similar: (i) self-fertilization reduces the parameter space in which male-benefit alleles can invade, thereby increasing opportunity for spread of female-benefit alleles (e.g., contrast fig. 2*A* with fig. 2*C*), and (*ii*) dominance

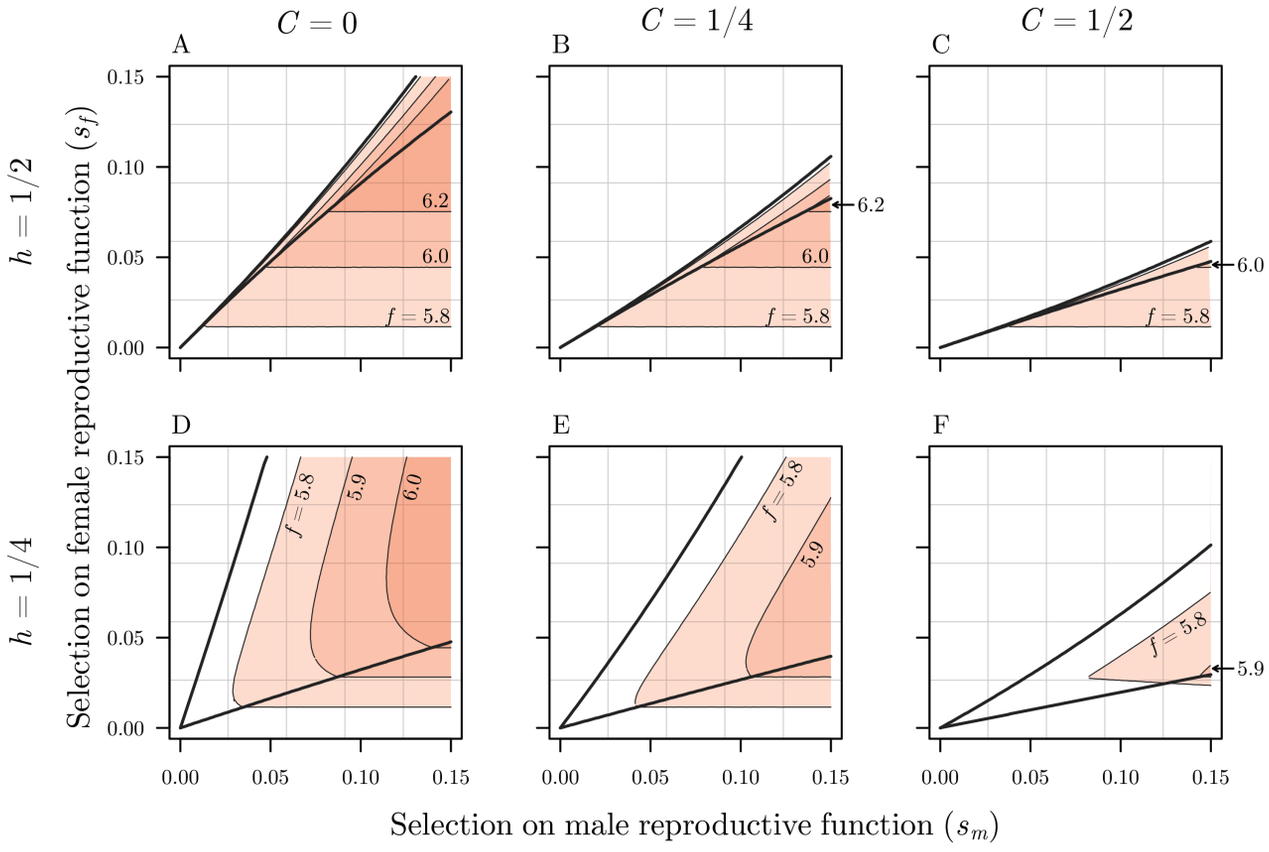

Figure 2: Illustration of parameter space for sexually antagonistic (SA) polymorphism and extinction thresholds predicted by the model. Balanced SA polymorphisms can be maintained in the funnel-shaped region between the invasion conditions for each SA allele (dark solid lines). However, for some parameter conditions, populations will ultimately become extinct (red regions) because of reduced female fitness resulting from the male-beneficial/female-deleterious allele that either segregates as a balanced polymorphism (inside the funnel) or becomes fixed (area below the funnel). Demographically viable polymorphic parameter space corresponds to the area inside the funnel that is also to the left of the extinction threshold for a given maximum female fertility value. Results are shown for three different population selfing rates ($C = \{0, 1/4, 1/2\}$) and two dominance scenarios (additivity, where $h = 1/2$, and dominance reversal, where $h = 1/4$). Extinction thresholds are illustrated for three different values of female fecundity (f values annotated on each panel); the coexistence boundaries are unaffected by the change in f. Surface plots of predicted population intrinsic growth rates (λ) for the same parameter conditions are presented as figure S1 in section S5 of the supplemental PDF.

reversals (where deleterious SA fitness effects are partially recessive in each sex; $h = 1/4$) are much more permissive of SA polymorphism (e.g., contrast fig. 2*A*–2*C* with fig. 2*D*–2*F*; Jordan and Connallon 2014; Olito 2017).

However, a key prediction from the evolutionary demographic model is that large fractions of SA polymorphic parameter space can be demographically inviable (fig. 2). The location of the extinction threshold, where the population intrinsic growth rate $\lambda = 1$, is primarily determined by the fertility parameter (f) but is also influenced by the population selfing rate (C) and dominance of the SA alleles (h).

In populations with high fertility (larger f), the proportion of demographically viable polymorphic parameter space converges on the predictions for total SA polymorphic space in population genetic models (fig. 3). In obligately outcrossing populations (including dioecious/gonochoristic populations, where $C = 0$), lower fertility can result in a significant reduction of demographically viable polymorphic parameter space. The effect is weaker in populations with intermediate selfing rates (compare $C = 0$ vs. $C > 0$) because self-fertilization generates a greater proportion of offspring that are homozygous for the female-beneficial allele relative to heterozygotes. In other words, self-fertilization reduces the opportunity for selection favoring the female-deleterious allele, thereby reducing the equilibrium load on female fecundity and allowing partially selfing populations to remain viable under selection intensities that would cause extinction in an outcrossing population. The combination of protection from reduced female fertility and reduced total polymorphic parameter

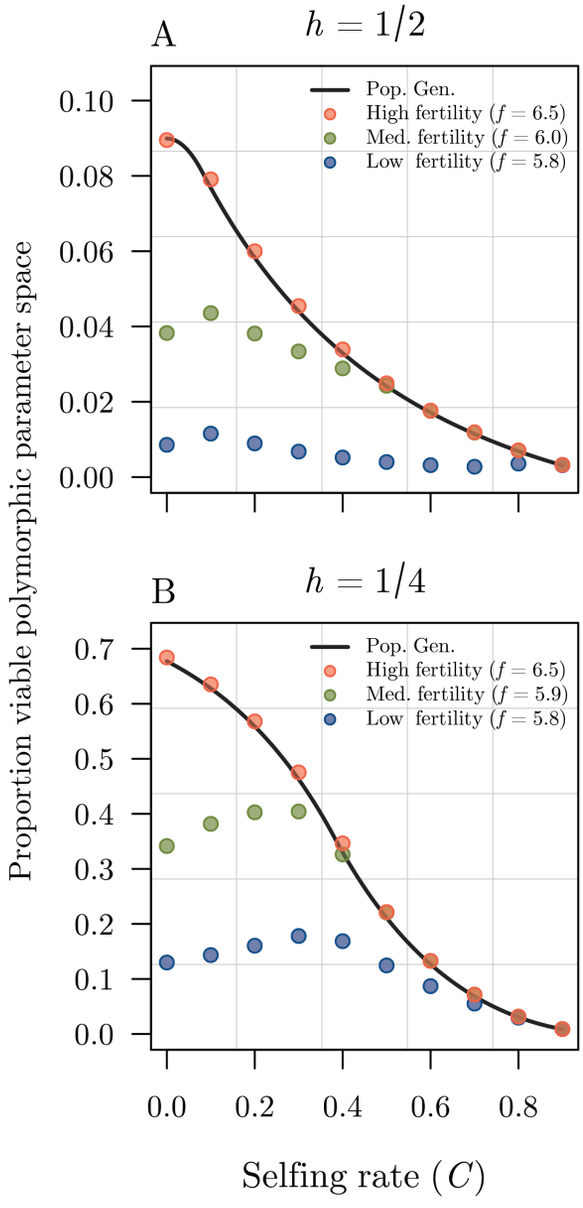

Figure 3: Proportion of demographically viable parameter space (out of total $s_f \times s_m$ space with $\max(s) = 0.15$) in the absence of inbreeding depression (i.e., assuming $\delta = \delta_i = 0$, where $i \in \{j, a, \gamma\}$), plotted as a function of the population selfing rate. Results are shown for three maximum female fertility values corresponding to low, medium, and high fertility (blue, green, and red points, respectively) under additive ($h = 1/2$; *A*) and partially recessive ($h = 1/4$; *B*) sexually antagonistic (SA) fitness effects. Each point was calculated by numerical integration of the corresponding SA invasion conditions and extinction threshold predicted by the Mendelian matrix model (see "Analyses"), while solid lines were produced by numerically integrating the analytic expressions for the single-locus invasion conditions from the population genetic models of Jordan and Connallon (2014) and Olito (2017; solid black lines).

space caused by selfing results in populations with intermediate selfing rates having the greatest proportion of demographically viable parameter space at medium and low fertilities (fig. 3, medium and low fertility values).

Demographic Effects of Inbreeding Depression

Unlike previous population genetic models of SA selection in hermaphrodites, which assume constant population sizes (Jordan and Connallon 2014; Olito 2017), mortality caused by inbreeding depression can strongly influence population persistence in our evolutionary demographic model. Populations with high fertility rates can maintain positive population growth rates despite this additional mortality. This causes a greater proportion of SA polymorphic parameter space to be demographically viable, with the demographic model predictions converging on those from population genetic models in high-fertility populations (fig. 4). Note, however, that mortality due to late-acting inbreeding depression also reduces the population effective selfing rate in our model and therefore shifts the invasion boundaries for the SA alleles to more closely resemble an outcrossing population. In some cases, this leads to larger regions of viable polymorphic space than predicted by the population genetic models, which include only early-acting inbreeding depression (e.g., see cross symbols in fig. 4). However, as the selfing rate increases, demographic viability eventually crashes when the population can no longer sustain the concomitant increase in mortality due to inbreeding depression (fig. 4).

Mortality from inbreeding depression quickly outweighs the beneficial effect of selfing on the equilibrium female load that was apparent in the previous section. In contrast to our earlier results, predominantly outcrossing populations are predicted to have the highest proportion of demographically viable polymorphic space when inbreeding depression is taken into account (compare fig. 3 with fig. 4). Regardless of the life history stage at which inbreeding depression affects survival, populations with intermediate to high selfing rates are unlikely to harbor SA polymorphism unless they can afford the resulting loss of self-fertilized ovules/offspring. An interesting alternative interpretation of these results is that populations with intermediate to high selfing rates and population intrinsic growth rates near 1 are vulnerable to extinction if a SA allele invades the population.

The point in the life cycle where inbreeding depression manifests can influence the threshold selfing rate at which demographically viable polymorphic parameter space crashes. Our results indicate that population viability was most sensitive to inbreeding depression affecting juvenile survival rates (δ_j; fig. 4, dark blue points), while early-acting inbreeding depression (δ, ovule abortion shortly after

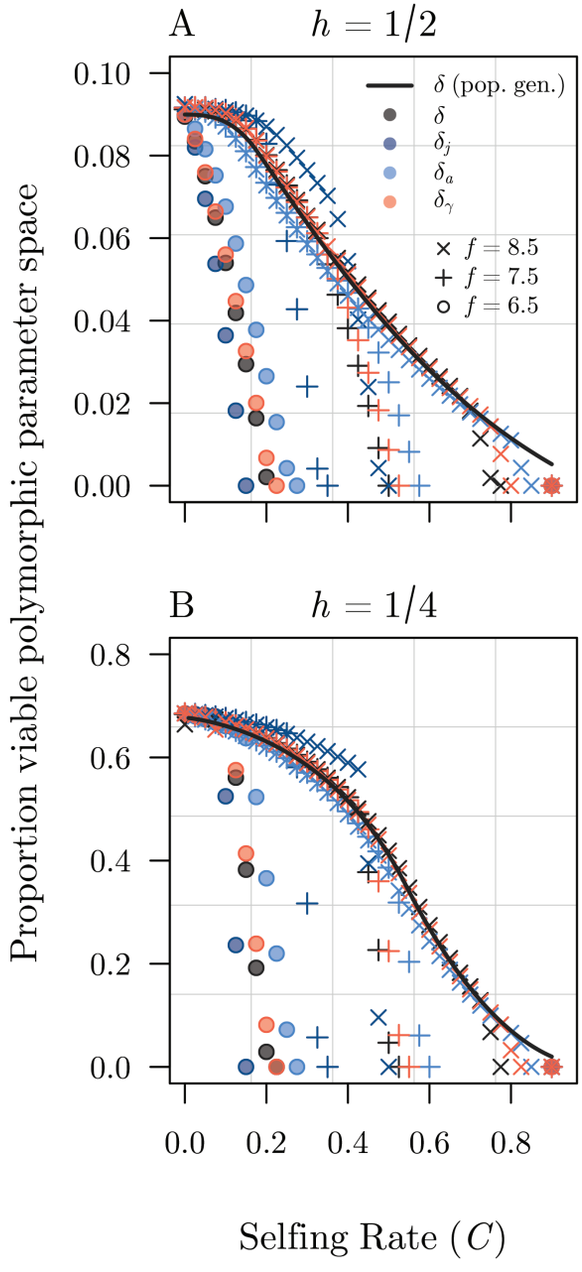

Figure 4: Effects of early- and late-acting inbreeding depression on the proportion of demographically viable parameter space (out of total $s_f \times s_m$ space with $\max(s) = 0.15$), plotted as a function of the population selfing rate. In all plots, the strength of inbreeding depression decreases as the selfing rate goes up following a simple model of purging recessive deleterious mutations (see "Analyses"). Only single inbreeding depression terms (δ and δ_i, where $i \in \{j, a, \gamma\}$, indicated in the legend) are allowed to vary at one time (all others are set to zero). Results are shown for three maximum female fertility values ($f = \{6.5, 7.5, 8.5\}$) under additive ($h = 1/2$; *A*) and partially recessive ($h = 1/4$; *B*) sexually antagonistic (SA) fitness effects. Each point was calculated by numerically integrating the corresponding SA invasion conditions and extinction threshold predicted by the model (see "Analyses"), while solid lines were produced by numerically integrating the single-locus invasion conditions from the population genetic models of Jordan and Connallon (2014) and Olito (2017; solid black lines).

fertilization) had a similar effect on population viability as late-acting inbreeding depression affecting adult survival (δ_a) and juvenile-to-adult transition rates (δ_γ). Inbreeding effects on juvenile survival had the strongest effect on population viability because, on average, individuals spend multiple time steps as juveniles before they mature. At each time step, juveniles mature with probability γ and survive with probability $\sigma_j(1 - \delta_j)$. Inbreeding depression at the juvenile stage therefore makes it harder to survive long enough to mature. Of course, the strength of this effect is influenced by the maturation rate, γ, which therefore also affects the shape of the curves in figure 4. Although early-acting inbreeding depression (δ) manifests earlier in the life cycle than juvenile survival, it acts only once, by influencing the total number of self-fertilized zygotes that become juveniles. Note, however, that the relative strength of inbreeding depression at different stages of the life history will depend on the interaction between the various inbreeding depression parameters, which we have precluded from our analyses.

Case Study: *Mimulus guttatus*

To illustrate how our model can be used to explore whether natural populations are likely to harbor balanced SA polymorphisms, we parameterized our model using empirically estimated demographic rates and fitness data for natural populations of the hermaphroditic flowering plant *M. guttatus* (Scrophulariaceae; now known as *Erythranthe guttata*). *Mimulus guttatus* is an herbaceous, self-compatible wildflower native to western North America that exhibits remarkable among-population variation in numerous life history and reproductive traits, including selfing rates, inbreeding depression, floral morphology, and annual-to-perennial life history (e.g., Ritland and Ganders 1987; Ritland 1990; Willis 1993, 1999*a*, 1999*b*; Wu et al. 2008). Moreover, detailed demographic studies have been conducted on multiple populations of *M. guttatus*, with demographic data available on the public demographic database COMPADRE (2020). Below, we briefly outline how we parameterized our model using the available data; full details are provided in section S6 of the supplemental PDF.

Demographic and Fitness Data for M. guttatus

To parameterize our model, we utilize extensive demographic data reported in a large-scale study of local adaptation using experimental populations of *M. guttatus* in Stanislaus National Forest (California) in 2012 and 2013

(Peterson et al. 2016). We leverage their common garden experimental design to focus on a comparison of the consequences of SA selection for two experimental populations with contrasting demographic rates. The first was a locally adapted Eagle Meadows population (data from 2012), while the second was an experimental population composed of multiple nonlocally adapted low-elevation perennials (data from 2013). The vital rate estimates for the Eagle Meadows population are as follows: seed bank survival ($D = 0.534$), seed germination rate ($G = 0.469$), flower production ($F = 0.64$), ovules per flower ($O = 614$), seedling recruits proportional to clonal rosette recruits ($A = 6.7 \times 10^{-4}$), overwinter survival ($S = 0.179$), and rosette production ($R = 8.71$). The corresponding estimates for the low-elevation perennials are $G = 0.652$, $F = 4.09$, $O = 494$, $S = 0$, and $R = 0$ (see corrected tables 1 and S2 in Peterson et al. 2017). The same estimates for D and A were used for all populations. The resulting transition matrices for this population involved three life history stages ($\omega = 3$; seed, seedling, and rosette), and individual elements of the transition matrix ($\tilde{\mathbf{A}}$) were calculated as products of the above rates (see matrix 1 in Peterson et al. 2016; also see eq. [S6.1] in sec. S6 of the supplemental PDF).

Estimates of selfing rates and inbreeding depression were not available for the same experimental populations but are available for a variety of other western US *M. guttatus* populations. Selfing rate estimates vary in magnitude from near complete outcrossing to predominant selfing ($C \approx 0$ to 0.75; Ritland and Ganders 1987; Ritland 1990; Willis 1999*a*). Estimates of inbreeding depression at several of the life history stages/fitness components that were included in the data of Peterson et al. (2016) are available for two intensively studied populations in the Cascade Mountains of Oregon (Iron Mountain and Cone Peak; Willis 1993, 1999*a*, 1999*b*). Using the data provided in Willis (1993), we estimated the proportional decrease due to inbreeding depression in seed germination rate ($\delta_G = 0.085$), flower number ($\delta_F = 0.2$), and overwinter survival ($\delta_S = 0.38$). The largest field-estimated selfing rate for the Iron Mountain population was $C = 0.29$ (Willis 1993).

Using these combined demographic rates, selfing rates, and inbreeding depression estimates, we constructed a corresponding stage × genotype Mendelian matrix model with a single SA locus affecting female and male fertility (as described above). With the empirically parameterized model, we are able to make predictions about the genetic and demographic outcome of SA selection at a single locus in hypothetical populations with the same demographic rates as observed in Peterson et al. (2016), for a range of selfing and inbreeding depression rates observed in other natural populations. We stress, however, that these are illustrative rather than explicit predictions of the likelihood of SA polymorphism in any specific population, and they ignore measurement error for the estimated demographic rates.

Interestingly, a polymorphic chromosomal inversion (inv6) with apparently SA fitness effects has been identified in the Iron Mountain population of *M. guttatus* (Lee et al. 2016). inv6 segregates at moderate frequency (about 8%), and carriers suffer an approximately 30% loss in pollen viability but also increased flower (and therefore ovule and pollen) production. The genetic basis of these effects remain unclear (although they are likely polygenic), but the net result is a supergene with remarkably strong effects on both female and male fertility that segregates as a single diallelic locus (i.e., with two alleles: wild type and inverted). We estimated selection coefficients for the effect of inv6 on pollen production (i.e., taking into account the simultaneous effect on flower number) and ovule production from the data reported in Lee et al. (2016) under the relatively conservative assumptions that pollen/ovule production is proportional to flower number and additive SA fitness effects (dominance coefficients could not be estimated from field data; see sec. S6 of the supplemental PDF for details). Under these assumptions, the average selection coefficient for inv6 on flower production across 2 years in the field was $(s_f, s_m) = (0.3, 0.31)$. As a final proof of concept for our empirically parameterized model (e.g., Servedio et al. 2014), we asked whether, given the above-described biologically grounded fitness effect estimates, inv6 appears to fall in demographically viable SA polymorphic parameter space (see fig. 5), as might be expected given its observed frequency in the Iron Mountain population.

Polymorphism in M. guttatus

The Eagle Meadows and low-elevation perennial populations of Peterson et al. (2016) had contrasting demographic rates that strongly affected the scope for demographically viable SA polymorphism. The locally adapted Eagle Meadows population had a very high intrinsic growth rate ($\lambda \approx 1.7$). This growth rate was sufficiently high that all $s_f \times s_m$ selection parameter space (where $s_f, s_m \in (0, 1]$) remained demographically viable, regardless of the selfing rate and effects of inbreeding depression ($C = 0$ or 0.29; fig. 5*A*, 5*C*). In contrast, the low-elevation perennial population had a much lower, but still positive, intrinsic growth rate ($\lambda \approx 1.08$). Because of the slower growth rate, not all of the $s_f \times s_m$ selection parameter space was demographically viable: extinction thresholds appear under both complete outcrossing and partial selfing with inbreeding depression (fig. 5*B*, 5*D*).

Whether under obligate outcrossing or partial selfing, inv6 always falls squarely in SA polymorphic space when

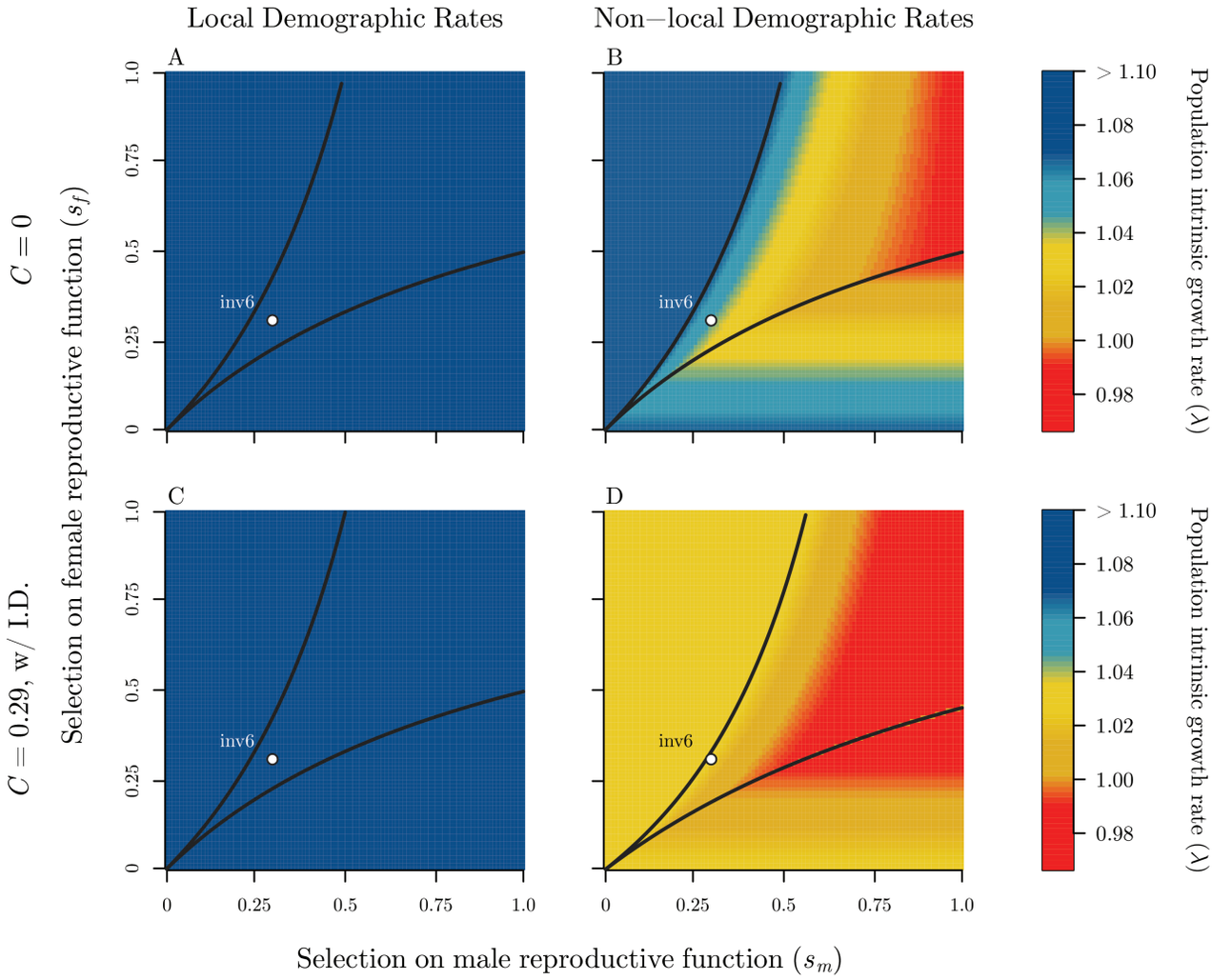

Figure 5: Illustration of model predictions using empirically estimated demographic rates for *Mimulus guttatus*. Results are shown for two hypothetical populations using demographic rates for locally adapted (Eagle Meadows; *A*, *C*), and nonlocal (low-elevation perennial; *B*, *D*) populations reported by Peterson et al. (2016). Invasion conditions and population intrinsic growth rates (λ) were calculated using the conservative assumption of additive fitness effects in both sexes ($h_f = h_m = 0.5$) for two parameter conditions: obligate outcrossing (*A*, *B*) and partial selfing with inbreeding depression using the highest field estimate of selfing and inbreeding depression parameters (δ_i) calculated for the Iron Mountain population of Willis (1993; *C*, *D*). The location of inv6 is also shown on both plots, using selection coefficients calculated from field estimates of male and female fitness components from Lee et al. (2016): $(s_f, s_m) = (0.30, 0.31)$.

using the locally adapted Eagle Meadows demographic rates (fig. 5*A*, 5*C*). In contrast, when the selfing rate is at the higher end of empirical estimates for the Iron Mountain population in which inv6 has been documented ($C = 0.29$), inv6 falls nearer the upper boundary but still within SA polymorphic space when using the low-elevation perennial demographic rates (fig. 5*B*, 5*D*). This happens because under the empirical estimates of selfing and inbreeding depression, the polymorphic parameter space shifts downward toward the *x*-axis. Additionally, inv6 falls much closer to the extinction threshold under partial selfing, suggesting that even relatively small perturbations to demographic rates or selection coefficients could result in nonlocally adapted populations being unable to support the demographic costs associated with segregating SA alleles with selection coefficients of similar magnitude to inv6.

We reanalyze this *M. guttatus* example using a simple density-dependent version of our model in section S3 of the supplemental PDF. We find that for (st)age-independent density-dependent growth, the coexistence boundaries are unchanged, and the equilibrium population densities

closely resemble the shape of the density-independent population growth rates presented above (see fig. S2.1).

Discussion

Classic population genetics theory predicts that SA selection can maintain genetic variation only under narrow conditions, with polymorphism requiring either finely balanced or unusually strong selection or partially recessive fitness effects through each sex (Kidwell et al. 1977; Pamilo 1979; Prout 2000; Connallon and Clark 2014). Extensions of the theory have identified numerous ways in which the conditions for polymorphism become more permissive in both dioecious and hermaphroditic organisms, including genetic linkage of SA loci, the evolution of sex-specific dominance, population subdivision, and life cycle complexity (e.g., Patten et al. 2010; Jordan and Charlesworth 2012; Jordan and Connallon 2014; Spencer and Priest 2016; Olito et al. 2018; Connallon et al. 2019). However, by ignoring the demographic consequences of SA genetic variation, these population genetic models have missed the possibility that SA polymorphisms may not be viable under realistic parameter conditions and are therefore unlikely to be observed in natural populations. By linking the individual-level fitness consequences of SA selection to population-level consequences, our theoretical framework provides several key insights into the processes shaping SA genetic variation in natural populations.

The first and central finding of our study is that when population intrinsic growth rates approach 1, the deleterious effects of segregating male-beneficial SA alleles on female fecundity can result in extinction over much of the parameter space where SA polymorphism is maintained. Additionally, large regions where male-beneficial alleles are predicted to fix become demographically inviable for populations whose intrinsic growth rates are close to 1 prior to invasion. This demographic consequence of masculinization has rarely been considered (Hitchcock and Gardner 2020). Since intrinsic growth rates far exceeding 1 suggest rapid exponential growth, they are generally rare (with the notable exceptions of recently introduced invasive populations), suggesting that our model predictions may be highly relevant for SA polymorphism in many real-world populations. Moreover, these findings complement recent theoretical and empirical studies indicating that SA selection is likely to be both condition dependent and stronger in locally adapted populations near the center of a species' range, where population fertility rates are expected to be higher and populations might be more likely to be able to suffer the demographic cost of a SA polymorphism while remaining viable (Berger et al. 2014; Connallon 2015).

We also find that demographically viable parameter space is often biased toward alleles with stronger selection through the female than male sex function. That is, given natural variation in population growth rates, the most demographically viable (and therefore observable in natural populations) outcomes of SA selection are either fixation of a female-beneficial allele or polymorphisms involving low-frequency female-deleterious alleles. This key prediction is supported by a series of experimental results in seed beetles (*Callosobruchus maculatus*), which show that male-beneficial SA genotypes are less likely to contribute positively to population growth rates and are more susceptible to extinction under environmental stress or inbreeding (Berger et al. 2014, 2016; Grieshop et al. 2017). An interesting corollary of our findings is that since strong SA fitness effects can often lead to extinction, the observable SA genetic variation in natural populations may often be under weak selection and therefore strongly susceptible to genetic drift, regardless of whether selection favors the fixation of one allele or polymorphism (Connallon and Clark 2012).

In hermaphroditic populations, self-fertilization can alleviate the demographic costs of balanced SA polymorphisms under some conditions; however, our model indicates that the concomitant effects of inbreeding depression will generally exacerbate them in populations with mixed-mating systems. This prediction is in stark contrast to previous population genetics models of SA selection in hermaphrodites, where the sole effect of inbreeding depression is to reduce the population effective selfing rate through the loss of selfed zygotes, thereby expanding polymorphic parameter space (Jordan and Connallon 2014; Olito 2017). In our model, this reduction in the effective selfing rate is accompanied by significant mortality due to inbreeding depression (whether early or late acting), which can quickly tip partially selfing populations over the brink to extinction. Beyond the maintenance of SA polymorphisms, this finding underscores a simple but important point that is often overlooked in studies of the evolution of self-fertilization, which tend to emphasize the coevolution of the deleterious mutation load and mating system (e.g., Lande and Schemske 1985; Charlesworth and Charlesworth 1987; Goodwillie et al. 2005): highly fertile populations can better afford the severe demographic costs of inbreeding. Thus, traits related to female fecundity, such as ovule and flower production, may strongly influence the distribution of successful transitions to self-fertilization among hermaphroditic taxa, along with other ecological correlates of selfing (Goodwillie et al. 2005; Igic and Kohn 2006; Grossenbacher et al. 2015).

Despite the demographic pitfalls associated with SA alleles, our case study using *Mimulus guttatus* appears to show that demographic rates observed in some real populations are capable of sustaining large regions of viable SA polymorphic space. The example also appears to provide some empirical support for the conjecture that locally

adapted populations are more likely to harbor SA polymorphisms than marginal or nonlocally adapted ones; inviable polymorphic parameter space only occurred when using the demographic data for nonlocal low-elevation perennial populations. Although we cannot make concrete predictions for inv6 in the Iron Mountain population in which it was observed, it is interesting that the estimated SA fitness effects place this polymorphic inversion squarely in demographically viable polymorphic parameter space predicted by our model. The available data do not allow for confident estimation of selection coefficients for inv6 (and even require making assumptions about dominance), yet our theoretical predictions are encouragingly consistent with the available data that inv6 is segregating at intermediate frequencies in the large and locally adapted Iron Mountain population.

Overall, our findings provide a more nuanced picture of the nature of SA genetic variation that we should expect to find in natural populations, where the fate of SA alleles and the populations harboring them is determined jointly by evolutionary and demographic processes.

Assumptions, Extensions, and Future Directions

By combining the tools of demography and population genetics, the framework we present here enables the exploration of interactions between life cycle complexity, mating system, and sexual antagonism. For the sake of simplicity, we made a variety of assumptions in our analyses, and many extensions of the model are possible. For example, we used a simple life cycle with just two stages for most of this article (the *Mimulus* example has three stages). However, it is possible to include additional age classes, allowing us to explore whether the scope for SA selection to maintain polymorphisms is affected by whether a species exhibits positive or negative senescence (Jones et al. 2014). Put another way, our model can be used to ask how the shape of the survival curve affects the demographic and population genetic consequences of SA selection and how this interacts with the age at which SA alleles are expressed, or what happens if SA alleles affect both male and female fertility and survival.

One particularly important limitation of our main analysis is that we modeled density-independent growth. Of course, in natural populations density-dependent processes like resource competition or competition for breeding sites will often prevent populations from growing (or shrinking) exponentially. In section S3 of the supplemental PDF, we incorporate a simple form of density dependence acting on the survival of all life history stages equally and reanalyzed our case study of *M. guttatus*. The density-dependent version of the model predicts equilibrium population densities rather than population intrinsic growth rates (see fig. S3.1). Our reanalysis shows that the shape of the polymorphic region is unchanged by this form of density dependence and that the population density surface in figure S3.1 is very similar to that for population growth rate in figure 5. The similarity between the density-independent and density-dependent model predictions underscores a key point made by earlier studies: density dependence acting (st)age independently does not alter selection gradients (Mylius and Diekmann 1995; Caswell and Shyu 2017).

Yet in many natural populations density dependence will not have the same effect on individual survival at all ages or developmental stages. For example, competition for breeding sites will cause a reduction in fecundity rather than survival. In plants, density-dependent competition for soil nutrients will influence seed germination rates differently than seedling growth rates or adult flower/fruit production (Antonovics and Levin 1980). These types of age- or stage-specific density dependence will change selection gradients and therefore the shape of polymorphic parameter space as well as the equilibrium population densities predicted by the model. De Vries et al. (2020) discuss some of the possible dynamical outcomes of a density-dependent genetic model for *Tribolium* seed beetles, but a thorough analysis of more complicated forms of density dependence for the maintenance of SA polymorphisms remains an important avenue for future work.

Like most demographic matrix models, ours assumed female demographic dominance, where population growth rates are determined entirely by female fecundity (Pollard 1975; Caswell 2001; Iannelli et al. 2005). Yet reproductive success in many hermaphroditic populations is limited by both the quantity and the quality of male gametes (e.g., Yund 2000; Aizen and Harder 2007; Harder et al. 2016). Modeling male gamete production is a natural extension to our framework and would enable us to analyze how tension between the demographic consequences of SA fitness variation through both female and male function alters or abolishes asymmetries in the extinction thresholds and polymorphic space caused from female demographic dominance (e.g., Tazzyman and Abbott 2015). Interestingly, different forms of self-fertilization can aid in reproductive assurance and should therefore have demographic consequences; for example, under pollen limitation and delayed selfing (where only ovules that fail to receive outcross pollen are selfed), the selfing rate will be a function of genotype frequencies because these will directly influence pollen production (Harder and Barrett 2006).

Our assumption that only how individuals themselves were produced (by selfing or outcrossing) affects the level of inbreeding depression they suffer also represents a major simplification. In reality, the history of consecutive generations of inbreeding in each individual's lineage will

influence the severity of inbreeding depression they experience, particularly when inbreeding depression is caused primarily by recessive deleterious mutations. It would be an interesting and feasible extension of our modeling framework to expand the individual state space to include selfing cohorts (i.e., first-generation selfing, second-generation selfing, etc.), as in Kelly (1999, 2007) and thereby provide a more biologically meaningful approach to modeling self-fertilization and inbreeding depression. Likewise, the simple fixed prior selfing model we implemented assumes constant selfing rates among individuals over time. In reality, environmental stochasticity will influence the population selfing rate and therefore both the expression of inbreeding depression and the scope for SA polymorphism (Jordan and Connallon 2014; Olito et al. 2018). A naive expectation might be that a weighted geometric mean selfing rate would represent a more biologically meaningful parameter influencing the genetic and demographic outcomes of SA selection in more complicated "selfing environments" (e.g., Connallon et al. 2019).

Finally, Grieshop et al. (2017) found that genotypes carrying male-beneficial SA alleles experience more severe inbreeding depression than those with female-beneficial SA alleles. This effect can easily be included in our model by making the inbreeding depression parameters, δ and δ_i, a function of the individual's genotype. Such SA genotype-dependent inbreeding depression would further reduce the demographically viable polymorphic parameter space and increase the bias in viable SA polymorphisms toward alleles with weaker selection in females.

Conclusions

Despite a surge of interest in eco-evolutionary dynamics, the demographic consequences of intralocus sexual antagonism have rarely been modeled (but see Kokko and Brooks 2003; Harts et al. 2014; Matthews et al. 2019). In contrast, models of the population dynamical consequences of interlocus sexual conflict are more common (e.g., Tanaka 1996; Martínez-Ruiz and Knell 2017). We found that including basic demography can have a significant impact on traditional population genetic results, as has been suggested previously by both theoretical and empirical studies (Kokko and Brooks 2003; Berger et al. 2016; Grieshop et al. 2017).

Demographic models connect individual-level traits to population-level consequences. As a consequence of their focus on individuals, demographic models are ideal for linking theory to experimental or field data, as demonstrated with our *Mimulus* case study. Doing so allows the field of population genetics to move from fitness as an abstract scalar metric toward the fitness of an entire life cycle, as calculated from observed rates of age- or stage-specific survival and fecundity.

Acknowledgments

We are grateful to the organizers and participants of the European Society for Evolutionary Biology (ESEB) Special Topics Network "Linking Local Adaptation with the Evolution of Sex Differences," where this collaboration was born. J. K. Abbott, T. Connallon, H. Caswell, S. F. van Daalen, C. Venables, the Genetics of Sex Research Group at Lund University, Editor Erol Akçay, A. E. Maria Orive, D. E. Robert Montgomerie, and two reviewers provided very helpful feedback on the manuscript. We are especially grateful to the editors for their efforts and patience during difficult times. This work was supported by a Wenner-Gren Foundation postdoctoral stipend to C.O. and by Swiss National Science Foundation grant 310030B_182836 and Academy of Finland grant 340130 (awarded to Jussi Lehtonen) to C.d.V.

Statement of Authorship

The authors jointly conceived the idea, refined the concepts, constructed the model, and wrote and edited the manuscript. C.O. performed the analyses and curated the digital repositories.

Data and Code Availability

A version of record for all data and computer code used in this study are publicly available on Zenodo (https://doi.org/10.5281/zenodo.6021025) and GitHub (https://github.com/colin-olito/SA-Hermaphrodites-wDemography).

Literature Cited

Abbott, J. K. 2011. Intra-locus sexual conflict and sexually antagonistic genetic variation in hermaphroditic animals. Proceedings of the Royal Society B 278:161–169.

Agrawal, A. F., and M. C. Whitlock. 2011. Inferences about the distribution of dominance drawn from yeast gene knockout data. Genetics 178:553–566.

Aizen, M., and L. Harder. 2007. Expanding the limits of the pollen-limitation concept: effects of pollen quantity and quality. Ecology 88:271–281.

Antonovics, J., and D. Levin. 1980. The ecological and genetic consequences of density-dependent regulation in plants. Annual Review of Ecology and Systematics 11:411–452.

Barfield, M., R. D. Holt, and R. Gomulkiewicz. 2011. Evolution in stage-structured populations. American Naturalist 177:397–409.

Berger, D., K. Grieshop, M. Lind, J. Goenaga, A. Maklakov, and G. Arnqvist. 2014. Intralocus sexual conflict and environmental stress. Evolution 68:2184–2196.

Berger, D., I. Martinossi-Allibert, K. Grieshop, M. I. Lind, A. A. Maklakov, and G. Arnqvist. 2016. Intralocus sexual conflict and the tragedy of the commons in seed beetles. American Naturalist 188:E98–E112.

Bonduriansky, R., and S. F. Chenoweth. 2009. Intralocus sexual conflict. Trends in Ecology and Evolution 24:280–288.

Caswell, H. 2001. Matrix models: construction, analysis, and interpretation. Sinauer, Sunderland, MA.

Caswell, H., and E. Shyu. 2017. Senescence, selection gradients and mortality. Pages 56–82 *in* R. P. Shefferson, O. R. Jones, and R. Salguero-Gomez. The evolution of senescence in the tree of life. Cambridge University Press, Cambridge.

Charlesworth, B. 1994. Evolution in age-structured populations. University of Chicago, Chicago.

Charlesworth, B., and K. A. Hughes. 2000. The maintenance of genetic variation in life history traits. Pages 369–391 *in* R. Singh and C. Krimbas, eds. Evolutionary genetics from molecules to morphology. Cambridge University Press, Cambridge.

Charlesworth, D. 1999. Theories of the evolution of dioecy. Pages 33–60 *in* M. A. Geber, T. E. Dawson, and L. F. Delph, eds. Gender and sexual dimorphism in flowering plants. Chap. 2. Springer Science and Business Media, Heidelberg.

Charlesworth, D., and B. Charlesworth. 1987. Inbreeding depression and its evolutionary consequences. Annual Review of Ecology and Systematics 18:237–268.

———. 2010. Elements of evolutionary genetics. Roberts, Greenwood Village, CO.

Charlesworth, D., and J. Willis. 2009. The genetics of inbreeding depression. Nature Reviews Genetics 10:783–796.

Childs, D. Z., B. C. Sheldon, and M. Rees. 2016. The evolution of labile traits in sex- and age-structured populations. Journal of Animal Ecology 85:329–342.

Chippindale, A., J. Gibson, and W. Rice. 2001. Negative genetic correlation for adult fitness between sexes reveals ontogenetic conflict in *Drosophila*. Proceedings of the National Academy of Sciences of the USA 98:1671–1675.

COMPADRE. 2020. Plant matrix database. https://www.compadre-db.org. Version 6.20.11.1.

Connallon, T. 2015. The geography of sex-specific selection, local adaptation, and sexual dimorphism. Evolution 69:2333–2344.

Connallon, T., and A. G. Clark. 2014. Balancing selection in species with separate sexes: insights from fisher's geometric model. Genetics 197:991–1006.

———. 2012. A general population genetic framework for antagonistic selection that accounts for demography and recurrent mutation. Genetics 190:1477–1489.

Connallon, T., and M. D. Hall. 2018. Genetic constraints on adaptation: a theoretical primer for the genomics era. Annals of the New York Academy of Sciences 1422:65–87.

Connallon, T., and G. Matthews. 2019. Cross-sex genetic correlations for fitness and fitness components: connecting theoretical predictions to empirical patterns. Evolution Letters 3:254–262.

Connallon, T., S. Sharma, and C. Olito. 2019. Evolutionary consequences of sex-specific selection in variable environments: four simple models reveal diverse evolutionary outcomes. American Naturalist 193:93–105.

Coulson, T., T. Benton, P. Lundberg, S. Dall, and B. Kendall. 2006. Putting evolutionary biology back in the ecological theatre: a demographic framework mapping genes to communities. Evolutionary Ecology Research 8:1155–1171.

Cox, R., and R. Calsbeek. 2009. Sexually antagonistic selection, sexual dimorphism, and the resolution of intralocus sexual conflict. American Naturalist 173:173–187.

Crnokrak, P., and S. Barrett. 2002. Purging the genetic load: a review of the experimental evidence. Evolution 56:2347–2358.

de Vries, C., and H. Caswell. 2019*a*. Selection in two-sex stage-structured populations: genetics, demography, and polymorphism. Theoretical Population Biology 130:160–169.

———. 2019*b*. Stage-structured evolutionary demography: linking life histories, population genetics, and ecological dynamics. American Naturalist 193:545–559.

de Vries, C., R. A. Desharnais, and H. Caswell. 2020. A matrix model for density-dependent selection in stage-classified populations, with application to pesticide resistance in *Tribolium*. Ecological Modelling 416:108875.

DeLisle, S., D. Goedert, A. Reedy, and E. Svensson. 2018. Climatic factors and species range position predict sexually antagonistic selection across taxa. Philosophical Transactions of the Royal Society B 373:20170415.

Delph, L. F., J. Andicoechea, J. Steven, C. Herlihy, S. Scarpino, and D. Bell. 2011. Environment-dependent intralocus sexual conflict in a dioecious plant. New Phytologist 192:542–552.

Eyre-Walker, A., and P. D. Keightly. 2007. The distribution of fitness effects of new mutations. Nature Reviews Genetics 8:610–618.

Fisher, R. A. 1930. The genetical theory of natural selection. Clarendon, Oxford.

Glémin, S. 2021. Balancing selection in self-fertilizing populations. Evolution 75:1011–1029.

Goodwillie, C., S. Kalisz, and C. G. Eckert. 2005. The evolutionary enigma of mixed mating systems in plants: occurrence, theoretical explanations, and empirical evidence. Annual Review of Ecology, Evolution, and Systematics 36:47–79.

Grieshop, K., D. Berger, and G. Arnqvist. 2017. Male-benefit sexually antagonistic genotypes show elevated vulnerability to inbreeding. BMC Evolutionary Biology 17:1–10.

Grossenbacher, D., R. Runquist, E. Goldberg, and Y. Brandvain. 2015. Geographic range size is predicted by plant mating system. Ecology Letters 18:706–713.

Harder, L. D., M. A. Aizen, and S. A. Richards. 2016. The population ecology of male gametophytes: the link between pollination and seed production. Ecology Letters 19:497–509.

Harder, L. D., and S. Barrett. 2006. Oxford University Press, Oxford.

Harder, L. D., and M. B. Routely. 2006. Pollen and ovule fates and reproductive performance by flowering plants. Pages 61–80 *in* L. D. Harder and S. C. H. Barrett, eds. Ecology and evolution of flowers. Chap. 4. Oxford University Press, Oxford.

Harts, A. M., L. E. Schwanz, and H. Kokko. 2014. Demography can favour female-advantageous alleles. Proceedings of the Royal Society B 281:20140005.

Hedrick, P., and A. Garcia-Dorado. 2016. An explicit model for the inbreeding load in the evolutionary analysis of selfing. Trends in Ecology and Evolution 31:940–952.

Hitchcock, T. J., and A. Gardner. 2020. A gene's-eye view of sexual antagonism. Proceedings of the Royal Society B 287:20201633.

Husband, B. C., and D. W. Schemske. 1996. Evolution of the magnitude and timing of inbreeding depression in plants. Evolution 50:54–70.

Iannelli, M., M. Martcheva, and F. A. Milner. 2005. Gender-structured population modeling: mathematical methods, numerics, and simulations. SIAM, Philadelphia.

Igic, B., and J. R. Kohn. 2006. The distribution of plant mating systems: study bias against obligately outcrossing species. Evolution 60:1098–1103.

Johnston, S. E., J. Gratten, C. Berenos, J. G. Pilkington, T. H. Clutton-Brock, J. M. Pemberton, and J. Slate. 2013. Life history trade-offs at a single locus maintain sexually selected genetic variation. Nature 502:93–95.

Jones, O. R., A. Scheuerlein, R. Salguero-Gómez, C. G. Camarda, R. Schaible, B. B. Casper, J. P. Dahlgren, et al. 2014. Diversity of ageing across the tree of life. Nature 505:169–173.

Jordan, C. Y., and D. Charlesworth. 2012. The potential for sexually antagonistic polymorphism in different genome regions. Evolution 66:505–516.

Jordan, C. Y., and T. Connallon. 2014. Sexually antagonistic polymorphism in simultaneous hermaphrodites. Evolution 68:3555–3569.

Kelly, J. K. 1999. Response to selection in partially self-fertilizing populations. I. Selection on a single trait. Evolution 53:336–349.

———. 2007. Mutation–selection balance in mixed mating populations. Journal of Theoretical Biology 246:355–365.

Kidwell, J. F., M. T. Clegg, F. M. Stewart, and T. Prout. 1977. Regions of stable equilibria for models of selection in the two sexes under random mating. Genetics 85:171–183.

Kokko, H., and R. Brooks. 2003. Sexy to die for? sexual selection and the risk of extinction. Annales Zoologici Fennici 40:207–219.

Lande, R. 1980. Sexual dimorphism, sexual selection, and adaptation in polygenic characters. Evolution 34:292–305.

Lande, R., and D. W. Schemske. 1985. The evolution of self-fertilization and inbreeding depression in plants. I. Genetic models. Evolution 39:24–40.

Lee, Y. W., L. Fishman, J. K. Kelly, and J. H. Willis. 2016. A segregating inversion generates fitness variation in yellow monkeyflower (*Mimulus guttatus*). Genetics 202:1473–1484.

Levene, H. 1953. Genetic equilibrium when more than one ecological niche is available. American Naturalist 87:331–333.

Lewis, Z., N. Wedell, and J. Hunt. 2011. Evidence for strong intralocus sexual conflict in the Indian meal moth, *Plodia interpunctella*. Evolution 65:2085–2097.

Lewontin, R. 1975. The genetic basis of evolutionary change. Columbia University Press, New York.

Lloyd, D. G., and C. J. Webb. 1986. The avoidance of interference between the presentation of pollen and stigmas in angiosperms. I. Dichogamy. New Zealand Journal of Botany 24:135–162.

Manna, F., G. Martin, and T. Lenormand. 2011. Fitness landscapes: an alternative theory for the dominance of mutation. Genetics 189:923–937.

Martínez-Ruiz, C., and R. J. Knell. 2017. Sexual selection can both increase and decrease extinction probability: reconciling demographic and evolutionary factors. Journal of Animal Ecology 86:117–127.

Matthews, G., S. Hangartner, D. G. Chapple, and T. Connallon. 2019. Quantifying maladaptation during the evolution of sexual dimorphism. Proceedings of the Royal Society B 286:20191372.

Mérot, C., V. Llaurens, E. Normandeau, L. Bernatchez, and M. Wellenreuther. 2020. Balancing selection via life-history tradeoffs maintains an inversion polymorphism in a seaweed fly. Nature Communications 11:1–11.

Metcalf, C. J. E., and S. Pavard. 2007. Why evolutionary biologists should be demographers. Trends in Ecology and Evolution 22:205–212.

Mylius, S., and O. Diekmann. 1995. On evolutionarily stable life histories, optimization, and the need to be specific about density dependence. Oikos 74:218–224.

Olito, C. 2017. Consequences of genetic linkage for the maintenance of sexually antagonistic polymorphism in hermaphrodites. Evolution 71:458–464.

Olito, C., J. K. Abbott, and C. Y. Jordan. 2018. The interaction between sex-specific selection and local adaptation in species without separate sexes. Philosophical Transactions of the Royal Society B 373:20170426.

Olito, C., and T. Connallon. 2019. Sexually antagonistic variation and the evolution of dimorphic sexual systems. American Naturalist 193:688–701.

Olito, C., and C. de Vries. 2022. The demographic costs of sexually antagonistic selection in partially selfing populations: simulation code and supplementary data. Zenodo, https://doi.org/10.5281/zenodo.6021025.

Orive, M. E. 1995. Senescence in organisms with clonal reproduction and complex life histories. American Naturalist 145:90–108.

———. 2001. Somatic mutations in organisms with complex life histories. Theoretical Population Biology 59:235–249.

Orive, M. E., M. Barfield, C. Fernandez, and R. D. Holt. 2017. Effects of clonal reproduction on evolutionary lag and evolutionary rescue. American Naturalist 190:469–490.

Pamilo, P. 1979. Genic variation at sex-linked loci: quantification of regular selection models. Hereditas 91:129–133.

Patten, M., D. Haig, and F. Úbeda. 2010. Fitness variation due to sexual antagonism and linkage disequilibrium. Evolution 64:3638–3642.

Peterson, M. L., K. M. Kay, and A. L. Angert. 2016. The scale of local adaptation in *Mimulus guttatus*: comparing life history races, ecotypes, and populations. New Phytologist 211:345–356.

———. 2017. Corrigendum. New Phytologist 216:956–957.

Pollard, J. H. 1975. Mathematical models for the growth of human populations. Cambridge University Press, Cambridge.

Prout, T. 1968. Sufficient conditions for multiple niche polymorphism. American Naturalist 102:493–496.

———. 2000. How well does opposing selection maintain variation? Pages 157–203 *in* R. S. Singh and C. B. Kimbras, eds. Evolutionary genetics from molecules to morphology. Cambridge University Press, Cambridge.

Rice, W. R. 1992. Sexually antagonistic genes: experimental evidence. Science 256:1436–1439.

Rice, W. R., and A. K. Chippindale. 2001. Intersexual ontogenetic conflict. Journal of Evolutionary Biology 14:685–693.

Ritland, K. 1990. Inferences about inbreeding depression based on changes of the inbreeding coefficient. Evolution 44:1230–1241.

Ritland, K., and F. R. Ganders. 1987. Covariation of selfing rates with parental gene fixation indices within populations of *Mimulus guttatus*. Evolution 41:760–771.

Ronce, O., S. Gandon, and F. Rousset. 2000. Kin selection and natal dispersal in an age-structured population. Theoretical Population Biology 58:143–159.

Roughgarden, J. 1971. Density-dependent natural selection. Ecology 52:453–468.

Rousset, F. 2004. Genetic structure and selection in subdivided populations. Vol. 40. Princeton University Press, Princeton, NJ.

Rueffler, C., M. Egas, and J. A. Metz. 2006. Evolutionary predictions should be based on individual-level traits. American Naturalist 168:E148–E162.

Ruzicka, F., L. Dutoit, P. Czuppon, C. Y. Jordan, X. Li, C. Olito, A. Runemark, E. I. Svensson, H. P. Yazdi, and T. Connallon. 2020. The search for sexually antagonistic genes: practical insights from studies of local adaptation and statistical genomics. Evolution Letters 4/5:398–415.

Ruzicka, F., L. Holman, and T. Connallon. 2022. Polygenic signals of sexually antagonistic selection in contemporary human genomes. bioRxiv, https://doi.org/10.1101/2021.09.20.461171.

Servedio, M. R., Y. Brandvain, S. Dhole, C. L. Fitzpatrick, E. E. Goldberg, C. A. Stern, J. Van Cleve, and D. J. Yeh. 2014. Not just a theory—the utility of mathematical models in evolutionary biology. PLoS Biology 12:e1002017.

Singh, A., and D. Punzalan. 2018. The strength of sex-specific selection in the wild. Evolution 72:2818–2824.

Spencer, H., and N. Priest. 2016. The evolution of sex-specific dominance in response to sexually antagonistic selection. American Naturalist 187:658–666.

Tanaka, Y. 1996. Sexual selection enhances population extinction in a changing environment. Journal of Theoretical Biology 180:197–206.

Tazzyman, S. J., and J. K. Abbott. 2015. Self-fertilization and inbreeding limit the scope for sexually antagonisitc polymorphism. Journal of Evolutionary Biology 28:723–729.

Wang, H., S. C. H. Barrett, X. Li, Y. Niu, Y. Duan, Z. Zhang, and Q. Li. 2021. Sexual conflict in protandrous flowers and the evolution of gynodioecy. Evolution 75:278–293.

Webb, C. J., and D. G. Lloyd. 1986. The avoidance of interference between the presentation of pollen and stigmas in angiosperms. II. Kerkogamy. New Zealand Journal of Botany 24:163–178.

Willis, J. H. 1993. Partial self-fertilization and inbreeding depression in two populations of *Mimulus guttatus*. Heredity 71:145–154.

———. 1999*a*. Inbreeding load, average dominance, and the mutation rate for mildly deleterious alleles in *Mimulus guttatus*. Genetics 153:1885–1898.

———. 1999*b*. The role of genes of large effect on inbreeding depression in *Mimulus guttatus*. Evolution 53:1678–1691.

Wu, C. A., A. M. Lowry, A. M. Cooley, K. M. Wright, Y. W. Lee, and J. H. Willis. 2008. *Mimulus* is an emerging model system for the integration of ecological and genomic studies. Heredity 100:220–230.

Yund, P. 2000. How severe is sperm limitation in natural populations of marine free-spawners? Trends in Ecology and Evolution 15:10–13.

References Cited Only in the Online Enhancements

Caswell, H. 2012. Matrix models and sensitivity analysis of populations classified by age and stage: a vec-permutation matrix approach. Theoretical Ecology 5:403–417.

Caswell, H., C. de Vries, N. Hartemink, G. Roth, and S. F. van Daalen. 2018. Age × stage-classified demographic analysis: a comprehensive approach. Ecological Monographs 4:88.

Charlesworth, B., and D. Charlesworth. 1978. A model for the evolution of dioecy and gynodioecy. American Naturalist 112:975–997.

Henderson, H. V., and S. R. Searle. 1981. The vec-permutation matrix, the vec operator and Kronecker products: a review. Linear Multilinear Algebra 9:271–288.

Hunter, C. M., and H. Caswell. 2005. The use of the vec-permutation matrix in spatial matrix population models. Ecological Modelling 188:15–21.

Magnus, J. R., and H. Neudecker. 1979. The commutation matrix: some properties and applications. Annals of Statistics 7:381–394.

Associate Editor: Maria E. Orive
Editor: Erol Akçay

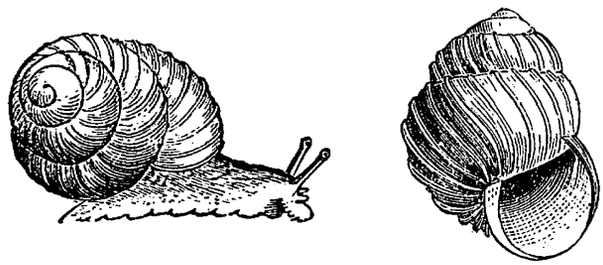

"Zoögenetes harpa *Say* . . . forms one of the few exceptions among land snails, in which the young are brought forth alive. They are hatched from eggs, but the eggs are retained within the parent when this process takes place." From "The Land Snails of New England (Continued)" by Edward S. Morse (*The American Naturalist*, 1868, 1:606–609).